

Monolayer NbF₄: a 4d¹-analogue of cuprates

Yang Yang,^{1,2} Wan-Sheng Wang,³ C. S. Ting,¹ and Qiang-Hua Wang^{4,5,*}

¹Texas Center for Superconductivity and Department of Physics,
University of Houston, Houston, Texas 77204, USA

²College of Physics and Electronic Engineering, Zhengzhou University of Light Industry, Zhengzhou, 450002, China

³Department of Physics, Ningbo University, Ningbo 315211, China

⁴National Laboratory of Solid State Microstructures & School of Physics, Nanjing University, Nanjing, 210093, China

⁵Collaborative Innovation Center of Advanced Microstructures, Nanjing University, Nanjing 210093, China

The electronic structure and possible electronic orders in monolayer NbF₄ are investigated by density functional theory and functional renormalization group. Because of the niobium-centered octahedra, the energy band near the Fermi level is found to derive from the 4d_{xy} orbital, well separated from the other bands. Local Coulomb interaction drives the undoped system into an antiferromagnetic insulator. Upon suitable electron/hole doping, the system is found to develop $d_{x^2-y^2}$ -wave superconductivity with sizable transition temperature. Therefore, the monolayer NbF₄ may be an exciting 4d¹ analogue of cuprates, providing a new two-dimensional platform for high- T_c superconductivity.

PACS numbers: : 74.20.-z, 74.20.Pq, 74.70.-b

Introduction: The search for high- T_c superconductors (HTS) has lasted for decades after the discovery of the cuprates[1]. A natural idea is to search for structural and electronic analogue of the cuprates, characterized by layered structure and a single energy band near the Fermi level derived from the d -orbital of the transition element. The correlation effect on top of the quasi two-dimensional (2D) band structure should make HTS very likely [2–8].

Recently, the infinite-layer nickelate NdNiO₂ has been discovered to be a superconductor with transition temperature $T_c = 9 \sim 15$ K upon doping[9]. As Cu²⁺ in cuprates, Ni²⁺ is in the 3d⁹ configuration, with 3d _{x^2-y^2} partially occupied. However, the hybridization with Nd-5d states near the Fermi level increases the complexity and possibly also limits the transition temperature.

Meanwhile, the development in 2D materials provides another avenue to find unconventional superconductors. Since the discovery of graphene[10, 11], many 2D materials have been explored for superconductivity (SC), such as doped phosphorene, single-layer B₂C, and 2D boron, *etc.*[12–15] Specifically, one of the most widely studied 2D superconductors is 2H-NbSe₂, where SC develops within the charge-density wave (CDW) phase[16]. It becomes more encouraging to search for new 2D superconductors after the observation of SC in the twisted bilayer graphene[17, 18] and high T_c SC in the one-unitcell monolayer Bi₂Sr₂CaCu₂O_{8+ δ} [19].

In this Letter we try to find a close 2D analogue of cuprates with non-copper transition element. The material we consider is the monolayer NbF₄, which has niobium-centered fluorine octahedra mimicing the oxygen octahedra in cuprates. By density functional theory (DFT) studies, we find a single band with dominant 4d_{xy} character near the Fermi level, while the other bands are well separated. Upon inclusion of the local Coulomb interaction, the parent compound is found to be an antifer-

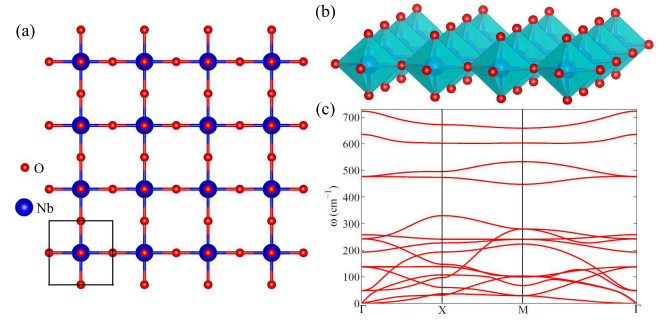


FIG. 1: (Color online) Crystal structures of monolayer NbF₄ from top view (a) and side view (b). The black solid lines denote the unit cell. (c) Phonon dispersion of monolayer NbF₄.

romagnetic insulator within DFT theory. By functional renormalization group (FRG) calculation on the basis of an effective Hubbard model, we find $d_{x^2-y^2}$ -wave SC upon electron/hole doping. These features make NbF₄ a promising and close analogue of cuprates, and may act as a new 2D platform for the exploration of HTS.

Crystal and DFT results: We start from the crystal structure of monolayer NbF₄. The crystallographic parameters are taken from Ref.[20]. The top view and side view of the crystal structure are shown in Fig.1(a) and (b), respectively. The Nb and F atoms form a square lattice and each Nb atom is centered in fluorine octahedra, resembling the oxygen octahedra surrounding copper ions in cuprates. The DFT calculations are performed using the Quantum ESPRESSO (QE) package[21]. The projected augmented wave (PAW) pseudopotentials with generalized gradient approximation (GGA) are adopted for the exchange-correlation energy[22].

The structures are fully relaxed until the force on each atom is < 0.001 eV/Å. After relaxation, the bond lengths between the Nb and F atoms is 2.07 Å (inplane) and

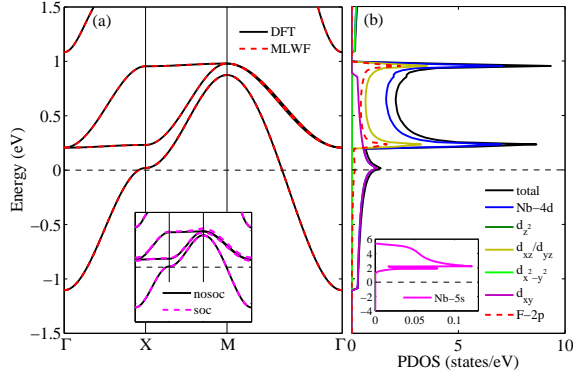


FIG. 2: (Color online) (a) Band structure obtained by DFT calculations (solid black lines) and MLWF fitting (dashed red lines) for NM state. The inset shows the comparison of band structure with and without SOC effect. (b) The total and partial DOS for monolayer NbF₄ in the NM state. The inset shows the PDOS of Nb-5s orbital.

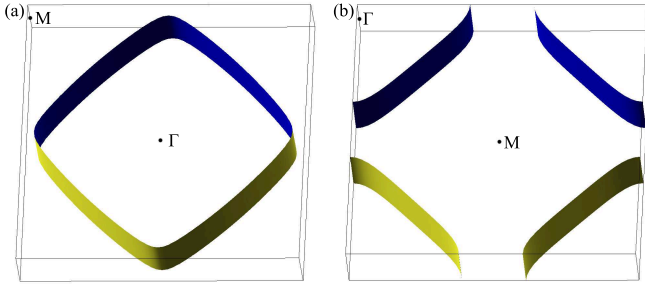


FIG. 3: (Color online) Fermi surface sheets of monolayer NbF₄ for NM state with $E_F = 0$ (a) and $E_F = 0.1\text{eV}$ (b), respectively.

1.87 Å(apical). For comparison, in cuprate the planer Cu-O bond length 1.96 Å and apical length 2.30 Å[23]. The fluorine octahedra can be seen as the oxygen octahedra rotated by 90 degrees. To confirm the thermodynamical stability of monolayer NbF₄, the phonon dispersion is further calculated. Fig.1(c) shows that no imaginary frequencies are observed in the phonon dispersion, indicating good kinetic stability of monolayer NbF₄. Besides, previous calculations have shown that the monolayer NbF₄ may be easily exfoliated from their parent compounds[20], encouraging the study of the monolayer.

We continue to discuss the electronic structure of monolayer NbF₄. As shown in Fig.2(a), there is only a single band crossing the Fermi level E_F . The partial density of states (PDOS) is shown in Fig.2(b). We see that the Nb-4d_{xy} plays a dominant role to the electronic states near E_F . In fact there is no apparent hybridization with the other 4d orbitals. On the other hand, the bands derived from F-2p are rather flat and mainly located -5.7 eV below the Fermi level (not shown), indicating negligible hybridization between F-2p and Nb-4d orbitals. The inset of Fig.2(b) shows the PDOS of Nb-5s, which

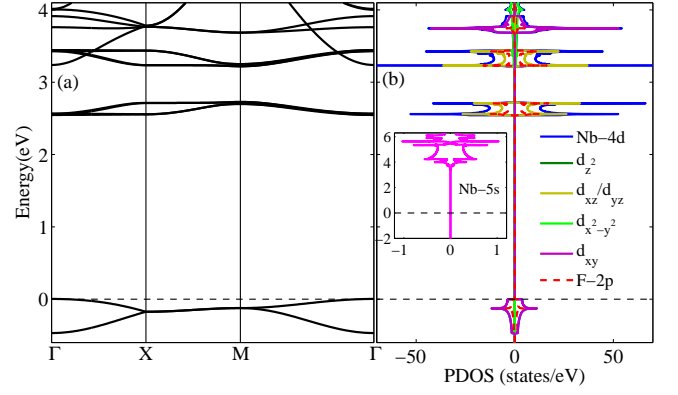


FIG. 4: (Color online) The band (a) and PDOS (b) of monolayer NbF₄ for G-type AFM state within GGA+U. The inset shows the PDOS of Nb-5s orbital in this case.

is above E_F hence unoccupied. Since the atomic configuration of Nb is $4d^45s^1$, intuitively the four electrons in the 4d-orbitals would be transferred to the four surrounding F⁻ ions. However, the PDOS shows that one electron in 5s- and three electrons in 4d-orbitals are lost instead, resulting in a half-filled 4d_{xy} orbital. This is in fact a natural effect of the crystal field: The compressed octahedra splits the 4d levels in the ascending order of d_{xy} , $d_{xz,yz}$, $d_{x^2-y^2}$ and $d_{3z^2-r^2}$, and also pushes up the 5s level, leaving d_{xy} the lowest level in the 4d and 5s levels. Therefore the Nb atom settles in the configuration close to $4d^1$. We also performed full-relativistic DFT calculations including spin-orbit coupling (SOC) effect. The comparison between the band structures with and without SOC are shown in the inset of Fig.2(a). No significant difference is found, especially near the Fermi level. Thus we shall not discuss the SOC effect henceforth for brevity.

The band near E_F with Nb-4d_{xy} character gives rise to remarkably simple FS sheets, as seen in Fig.3(a). A rounded-square FS around Γ point cuts the Brillouin zone into two parts of roughly the same size. Thus the FS are featured by a quasi-nesting vector (π, π) . Since this system is near half filling, the FS can evolve into either electron pockets around Γ point or hole pockets around M point by rigid band shift, resulting in Lifshitz transition. As an example, Fig.3(b) shows the FS evolves into a hole pocket around the M point when E_F is shifted upward by 0.1eV. There is a Van Hove singularity (VHS) in the vicinity of X point of the band dispersion, leaving a peak in DOS near E_F . The proximity to the VHS is similar to that in cuprates, making the system highly susceptible to electron instabilities when the interaction between electrons is taken into account.

Indeed, we obtain the magnetic ground state by employing DFT. The calculations are performed within both $2 \times 2 \times 1$ and $3 \times 3 \times 1$ supercells. We consider the nonmagnetic (NM) state, ferromagnetic (FM) state, G-type antiferromagnetic (AFM) state, and C-type AFM state. We

find the G-type AFM state is energetically favored, about 131.7 meV (per Nb atom) lower than the NM state. The magnetic moment estimated for the AFM state is about $0.38 \mu_B$ per Nb. Including the local coulomb interaction U , the G-type AFM state becomes 426.6 meV lower than the NM state, and the magnetic moment increases to about $0.44 \mu_B$.

We further perform GGA+ U calculation to incorporate the correlation effect better.[25] It is known that if the on-site Coulomb interaction is included in the AFM configurations, the electronic state of cuprates can become insulating. Instead, without the local interaction, the ground state is metallic, as demonstrated in recent studies of $\text{Ba}_2\text{CuO}_{3+\delta}$ [24]. In our calculation, we determine $U \sim 4.05$ eV using density-functional perturbation theory (DFPT) as implemented in QE[26], which is close to the former results[27, 28]. With this value of U in the G-type AFM configuration, the obtained bands and PDOS are shown in Fig.4(a) and (b), respectively. Obviously, the previous nonmagnetic metallic state now becomes AFM insulating. Differently from cuprates, the top of the valence band is located at the Γ point, and the band gap is ~ 2.5 eV, larger than that of Ca_2CuO_3 (1.7 eV) and Sr_2CuO_3 (1.5 eV)[29]. Owing to the $4d^1$ configuration, the PDOS of $4d_{xy}$ is splitted into two parts while the other four $4d$ orbitals are almost unaffected. Additionally, the Nb-5s remains unoccupied but more electrons are transferred from Nb- $4d_{xy}$ to F-2p, resulting in slightly stronger $p-d$ hybridization, as seen from the PDOS peaks of $4d$ and F-2p in Fig.4(b).

Since only Nb- $4d_{xy}$ orbital dominates the low energy physics in monolayer NbF_4 , it is rather easy to derive a single-orbital tight-binding model. Firstly, we obtain an effective model including five Nb- $4d$ orbitals by the maximally-localized Wannier function method[30, 31]. Then we obtain an effective single-orbital model to describe the electronic properties near E_F . The band dispersion in momentum space can be well approximated by

$$\begin{aligned} \epsilon_{\mathbf{k}} = & 2t_1(\cos k_x + \cos k_y) + 4t_2 \cos k_x \cos k_y \\ & + 2t_3[\cos(2k_x) + \cos(2k_y)] \\ & + 4t_4[\cos(2k_x) \cos k_y + \cos k_x \cos(2k_y)] - \mu, \end{aligned} \quad (1)$$

where $t_1 = -0.245$ eV, $t_2 = -0.017$ eV, $t_3 = 0.002$ eV, $t_4 = -0.001$ eV, and the chemical potential $\mu = 0.054$ eV in the undoped case. Note the hopping integral here follows from the direct overlap between d_{xy} orbitals, without having to be bridged by the $p_{x,y}$ -orbitals (which would be necessary for hopping between $d_{x^2-y^2}$ orbitals). This results in a relatively narrow band, of width ~ 2 eV, crossing E_F .

FRG analysis: The similarity in the electronic structures of monolayer NbF_4 and cuprate motivates us to consider the possibility of superconductivity in monolayer NbF_4 . We consider the Hubbard model with the

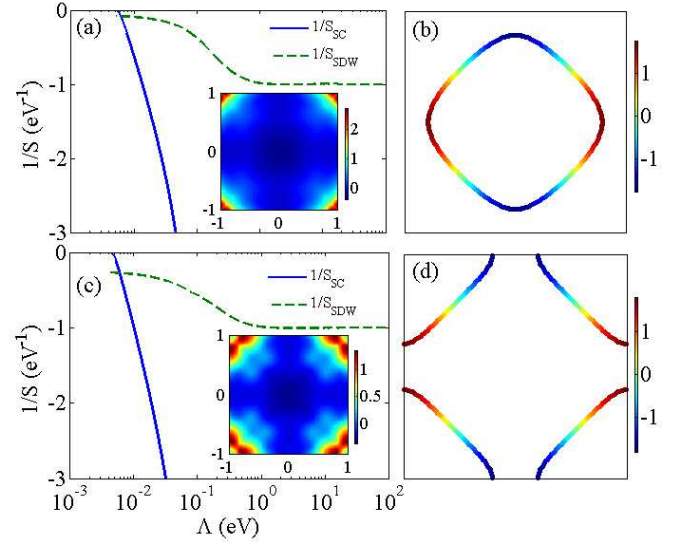


FIG. 5: (Color online)(a) FRG flow of $1/S_{SC,SDW}$ versus the running energy scale Λ for $n = 0.85$ and $U = 1.0$ eV. The inset shows $|S_{SDW}(\mathbf{q})|$ in the Brillouin zone at the final energy scale. (b) The Fermi surface and gap function $\Delta(\mathbf{k})$ (color scale). (c) (d) shows the FRG flow and gap function $\Delta(\mathbf{k})$ for $n = 1.26$ and $U = 1.0$ eV.

normal state described by Eq.1 and a local Hubbard interaction U . The interaction can lead to competing collective fluctuations that must be treated on equal footing. For this purpose, we use the singular-mode functional renormalization group (SMFRG) method[32–41]. In this method, the one-particle-irreducible four-point interaction vertex function Γ is calculated iteratively versus a decreasing energy scale Λ . During the FRG flow, we decompose Γ into scattering matrices in the basis of fermion bilinears (separately) in the pairing (SC), spin-density-wave (SDW) and CDW channels. The divergence of the negative leading eigenvalue (NLE) S of the scattering matrices signals an emerging order at the associated collective momentum, and the internal structure of the order parameter is described by the associated eigenfunction of the scattering matrix. The technical details can be found elsewhere[32–41].

We have performed systematic calculations by varying the filling level n and the local Coulomb interaction U . The maximum value of n is restricted ($n < 1.4$) to avoid the influence of the other $4d$ orbitals. We select two typical cases for illustration.

For hole doping with $n = 0.85$ and $U = 1$ eV, the FRG flow versus Λ is shown in Fig.5(a). Since the CDW channel remains weak during the flow, we shall not discuss it henceforth. From the flow, we find the SDW channel is enhanced in the intermediate stage, but becomes flat at low-energy scales because of lack of phase space for low-energy particle-hole excitations. The NLE of SDW channel S_{SDW} is associated with scattering momentum $\mathbf{Q} = (\pi, \pi)$ and remains almost unchanged dur-

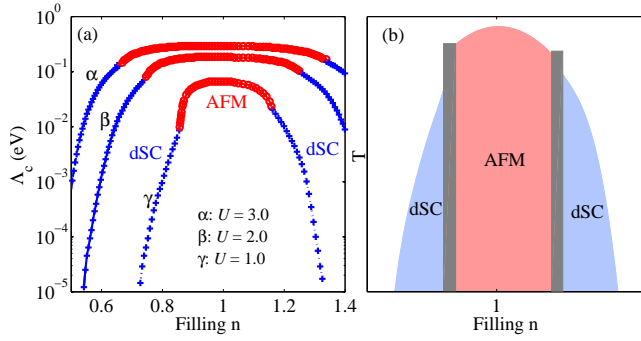


FIG. 6: (Color online)(a) The FRG diverging energy scale Λ_c plotted as a function of filling level n .(b) A schematic temperature-doping phase diagram near $n=1$. The gray region denotes the transition between SC and AFM.

ing the flow. The inset of Fig.5(a) shows $S_{\text{SDW}}(\mathbf{q})$ versus \mathbf{q} at the final stage, which is peaked around (π, π) . We checked that this scattering mode describes site-local spins, indicating strong AFM fluctuations consistent with the DFT results. Triggered by such spin fluctuations, the pairing interaction S_{SC} are enhanced and diverges at the final energy scale, indicating the system develops a SC instability. The pairing function, or the eigenfunction of the Cooper scattering eigen mode, is found to be $\cos k_x - \cos k_y$ with $d_{x^2-y^2}$ -wave symmetry. This symmetry is made explicit by the plot of the pairing function on the Fermi surface in Fig.5(b).

Similar calculations are performed for electron doping with $n = 1.26$ and $U = 1.0$ eV. The FRG flow and pairing gap on FS are presented in Fig.5(c) and (d), respectively. The leading scattering momentum in the SDW channel is (π, π) at high-energy scales and changes slightly at lower energy scale owing to the change of the FS topology. At the final stage, the $S_{\text{SDW}}(\mathbf{q})$ peaks at $\mathbf{Q} = (0.94, 0.81)\pi$, which is also near (π, π) , as shown in the inset of Fig.5(d). In the pairing channel, the pairing symmetry remains to be $d_{x^2-y^2}$. This is because the attractive pairing interaction is triggered by SDW fluctuations in the intermediate energy window, while the change of FS topology is important only for low-energy particle-hole excitations.

In Fig.6(a) we plot the divergence scale (representative of the transition temperature) in the AFM or SC channel, whichever is larger, as a function of the filling level n , for three values of U . The AFM order is favored near half filling ($n = 1$), and a larger U enlarges the AFM region significantly. The SC order is favored upon small electron/hole doping. We observe that near the phase boundary between AFM and SC, the divergence scale is sizable, ranging from 8 meV at $U = 1$ eV, to 100 meV at $U = 3$ eV. This suggests that the monolayer NbF_4 may be a HTS. On the basis of the above results, we draw a schematic phase diagram, Fig.6(b), for monolayer NbF_4 with a realistic local Coulomb interaction, of the order of the values we considered. The grayed region indicates

the transition between AFM and SC.

We should remark that since the d_{xy} -derived band is relatively narrow, it is likely that the system is close to or in the Mott limit. In that case, the SC regime in Fig.6(b) may become a dome, like that in cuprates. The Mott limit is unfortunately beyond the realm of FRG on the basis of itinerant normal state. Instead of the Hubbard model, a better starting point is the t - J model, which is however even more difficult to tackle reliably, although the same type of model has been studied extensively in the context of cuprates. We stress that our FRG within the Hubbard model provides qualitatively reliable result from weak to moderate coupling, and we leave the Mott limit in future studies.

Summary: The electronic structure and superconductivity of monolayer NbF_4 are investigated by DFT and FRG. A single band derived from $\text{Nb-}4d_{xy}$ orbital is found near the Fermi level. Near half filling the system is in the AFM state, while electron/hole doping introduces d -wave SC, potentially with high T_c . The structural and electronic similarity to that in cuprates makes monolayer NbF_4 an excellent $4d^1$ analogue of cuprates and a new platform to explore HTS.

Acknowledgments: The project was supported by the National Key Research and Development Program of China (under Grant No. 2016YFA0300401), the National Natural Science Foundation of China (under Grant Nos.11604303, 11604168 and 11574134), the Texas Center for Superconductivity at the University of Houston and the Robert A. Welch Foundation (Grant No. E-1146). YY acknowledges support by China Scholarship Council (under Grant No. 201909440001).

* Electronic address: qhwang@nju.edu.cn

- [1] J. G. Bednorz and K. A. Müller, Z. Phys. B **64**, 189 (1986).
- [2] R. Arita, K. Kuroki, and H. Aoki, Phys. Rev. B **60**, 14585 (1999).
- [3] R. Arita, K. Kuroki, and H. Aoki, J. Phys. Soc. Jpn. **69**, 1181 (2000).
- [4] P. Monthoux and G. G. Lonzarich, Phys. Rev. B **59**, 14598 (1999).
- [5] P. Monthoux and G. G. Lonzarich, Phys. Rev. B **63**, 054529 (2001).
- [6] H. Sakakibara, H. Usui, K. Kuroki, R. Arita, and H. Aoki, Phys. Rev. Lett. **105**, 057003 (2010).
- [7] H. Sakakibara, K. Suzuki, H. Usui, K. Kuroki, R. Arita, D. J. Scalapino, and H. Aoki, Phys. Rev. B **86**, 134520 (2012).
- [8] H. Sakakibara, H. Usui, K. Kuroki, R. Arita, and H. Aoki, Phys. Rev. B **85**, 064501 (2012).
- [9] D. Li, K. Lee, B. Y. Wang, M. Osada, S. Crossley, H. R. Lee, Y. Cui, Y. Hikita, and H. Y. Hwang, Nature **572**, 624 (2019).
- [10] K. S. Novoselov, A. K. Geim, S. V. Morozov, D. Jiang, Y. Zhang, S. V. Dubonos, I. V. Grigorieva, and A. A.

- Firsov, Science **306**, 666 (2004).
- [11] K. S. Novoselov, A. K. Geim, S. V. Morozov, D. Jiang, M. I. Katsnelson, I. V. Grigorieva, S. V. Dubonos, and A. A. Firsov, Nature **438**, 197 (2005).
 - [12] D. F. Shao, W. J. Lu, H. Y. Lv and Y. P. Sun, Europhys. Lett. **108**, 67004 (2014).
 - [13] J. Dai, Z. Li, J. Yang and J. Hou, Nanoscale **4**, 3032 (2012).
 - [14] Y. Zhao, S. Zeng and J. Ni, Phys. Rev. B **93**, 014502 (2016).
 - [15] E. S. Penev, A. Kutana and B. I. Yakobson, Nano Lett. **16**, 2522 (2016).
 - [16] X. Xi, L. Zhao, Z. Wang, H. Berger, L. Forr, J. Shan, and K. F. Mak, Nat. Nanotechnology **10**, 765 (2015).
 - [17] Y. Cao, V. Fatemi, S. Fang, K. Watanabe, T. Taniguchi, E. Kaxiras, and P. Jarillo-Herrero, Nature **556**, 43 (2018).
 - [18] Y. Cao, V. Fatemi, A. Demir, S. Fang, S. L. Tomarken, J. Y. Luo, J. D. Sanchez-Yamagishi, K. Watanabe, T. Taniguchi, E. Kaxiras, R. C. Ashoori, and P. Jarillo-Herrero, Nature **556**, 80 (2018).
 - [19] Y. Yu, L. Ma, P. Cai, R. Zhong, C. Ye, J. Shen, G. D. Gu, X. H. Chen, and Y. Zhang, Nature **575**, 156 (2019).
 - [20] N. Mounet, M. Gibertini, P. Schwaller, D. Campi, A. Merkys, A. Marrazzo, T. Sohier, I. E. Castelli, A. Cepellotti, G. Pizzi and N. Marzari, Nat. Nanotechnology **13**, 246-252 (2018).
 - [21] P. Giannozzi, *et al.*, J.Phys.:Condens.Matter, **21**, 395502 (2009).
 - [22] J. P. Perdew, K. Burke, and M. Ernzerhof, Phys. Rev. Lett. **77**, 3865 (1996).
 - [23] A. Bianconi, N. L. Saini, A. Lanzara, M. Messori, T. Rossetti, H. Oyanagi, H. Yamaguchi, K. Oka, and T. Ito, Phys. Rev. Lett. **76**, 3412 (1996).
 - [24] K. Liu, Z. Y. Lu, T. Xiang, Phy. Rev. Mat., **3**, 044802 (2019).
 - [25] S. L. Dudarev, G. A. Botton, S. Y. Savrasov, C. J. Humphreys, and A. P. Sutton, Phys. Rev. B **57**, 1505 (1998).
 - [26] I. Timrov, N. Marzari and M. Cococcioni, Phys. Rev. B **98**, 085127 (2018).
 - [27] E. Sasioglu, C. Friedrich, and S. Blügel, Phys. Rev. B **83**, 121101 (2011).
 - [28] L. Vaugier, H. Jiang, and S. Biermann, Phys. Rev. B **86**, 165105 (2012).
 - [29] K. Maiti, D. D. Sarma, T. Mizokawa, and A. Fujimori, Phys. Rev. B **57**, 1572 (1998).
 - [30] A. A. Mostofi, J. R. Yates, Y.-S. Lee, I. Souza, D. Vanderbilt, and N. Marzari, Comput. Phys. Commun. **178**, 685 (2008).
 - [31] A. A. Mostofi, J. R. Yates, G. Pizzi, Y.-S. Lee, I. Souza, D. Vanderbilt, and N. Marzari, Comput. Phys. Commun. **185**, 2309 (2014).
 - [32] W.-S. Wang, Y.-Y. Xiang, Q.-H. Wang, F. Wang, F. Yang, and D.-H. Lee, Phys. Rev. B **85**, 035414 (2012).
 - [33] Y.-Y. Xiang, W.-S. Wang, Q.-H. Wang, and D.-H. Lee, Phys. Rev. B **86**, 024523 (2012).
 - [34] Y.-Y. Xiang, F. Wang, D. Wang, Q.-H. Wang, and D.-H. Lee, Phys. Rev. B **86**, 134508 (2012).
 - [35] W.-S. Wang, Z.-Z. Li, Y.-Y. Xiang, and Q.-H. Wang, Phys. Rev. B **87** 115135 (2013).
 - [36] Y.-Y. Xiang, Y. Yang, W.-S. Wang, Z.-Z. Li, Q.-H. Wang, Phys. Rev. B **88**, 104516 (2013).
 - [37] Y. Yang, W.-S. Wang, Y.-Y. Xiang, Z.-Z. Li, Q.-H. Wang, Phys. Rev. B **88**, 094519 (2013).
 - [38] Q. H. Wang, C. Platt, Y. Yang, C. Honerkamp, F. C. Zhang, W. Hanke, T. M. Rice, R. Thomale, Europhys. Lett. **104**, 17013 (2013).
 - [39] Y. Yang, W.-S. Wang, J.-G. Liu, H. C., J.-H. Dai and Q.-H. Wang, Phys. Rev. B **89**, 094518 (2014).
 - [40] W.-S. Wang, Y. Yang, Q. H. Wang, Phys. Rev. B **90**, 094514 (2014).
 - [41] W.-S. Wang, C.-C. Zhang, F.-C. Zhang, and Q.-H. Wang, Phys. Rev. Lett. **122**, 027002 (2019).
 - [42] See the supplementary of Ref.[40] and Ref.[41].
 - [43] A. Liebsch and A. I. Lichtenstein, Phys. Rev. Lett. **84**, 1591 (2000).